Electrocochleography in Cochlear Implant Recipients: Correlating Maximum Response With Residual Hearing

Raphael R. Andonie,[1,2] Wilhelm Wimmer,[2,3] Stephan Schraivogel,[1,2] Georgios Mantokoudis,[2] Marco Caversaccio,[1,2] and Stefan Weder[2]

Objectives: Electrocochleography (ECochG) is increasingly recognized as a biomarker for assessing inner ear function in cochlear implant patients. This study aimed to objectively determine intraoperative cochlear microphonic (CM) amplitude patterns and correlate them with residual hearing in cochlear implant recipients, addressing the limitations in current ECochG analysis that often depends on subjective visual assessment and overlook the intracochlear measurement location.

Design: In this prospective study, we investigated intraoperative pure-tone ECochG following complete electrode insertion in 31 patients. We used our previously published objective analysis method to determine the maximum CM amplitude and the associated electrode position for each electrode array. Using computed tomography, we identified electrode placement and determined the corresponding tonotopic frequency using Greenwood's function. Based on this, we calculated the tonotopic shift, that is, the difference between the stimulation frequency and the estimated frequency of the electrode with the maximum CM amplitude. We evaluated the association between CM amplitude, tonotopic shift, and preoperative hearing thresholds using linear regression analysis.

Results: CM amplitudes showed high variance, with values ranging from −1.479 dB re 1 μV (to 4.495 dBμV. We found a statistically significant negative correlation ($p < 0.001$, $r = -0.62$ [−0.74, −0.45]) between maximum CM amplitudes and preoperative hearing thresholds. In addition, a significant association ($p < 0.001$, $r = 0.46$ [0.27, 0.62]) between the tonotopic shift and preoperative hearing thresholds was observed. Tonotopic shifts of the maximum CM amplitudes occurred predominantly toward the basal direction.

Conclusions: The combination of objective signal analysis and the consideration of intracochlear measurement locations enhances the understanding of cochlear health and overcomes the obstacles of current ECochG analysis. We could show the link between intraoperative CM amplitudes, their spatial distributions, and preoperative hearing thresholds. Consequently, our findings enable automated analysis and bear the potential to enhance specificity of ECochG, reinforcing its role as an objective biomarker for cochlear health.

Key words: Autonomous linear state-space models, Cochlear microphonic, Computed tomography, Electrocochleography, Objective algorithms, Residual hearing, Tonotopy.

Abbreviations: AID = angular insertion depth; CDL = cochlear duct length; CI = cochlear implant; CM = cochlear microphonic; CM-MR = cochlear microphonic maximum response; CT = computed tomography; ECochG = electrocochleography; LCR = logarithmic cost ratio; PTA = pure-tone average.

(Ear & Hearing 2024;XX;00–00)

INTRODUCTION

With the expansion of indications for a cochlear implant (CI), there is an increasing number of candidates exhibiting residual hearing (Hempel et al. 2018). Research shows that patients whose residual hearing can be preserved despite the surgery benefit from improved speech perception, sound localization, and music appreciation (Gifford et al. 2013; Sheffield et al. 2015; Gantz et al. 2022). Consequently, cochlear health monitoring during and after implantation is gaining importance. In this context, intracochlear electrocochleography (ECochG) recorded through the CI is increasingly used to assess cochlear health (Koka et al. 2017; Weder et al. 2020; Lenarz et al. 2022; Schuerch et al. 2022a; Bester et al. 2023; Walia et al. 2023).

ECochG measures acoustically evoked potentials emanating from neurosensory structures within the cochlea (Dallos et al. 1972). The cochlear microphonic (CM) is the largest and most commonly analyzed component of ECochG, primarily reflecting the activity of outer hair cells (Dallos & Cheatham 1976; Schuerch et al. 2022b). In a healthy cochlea, due to its tonotopic organization, the maximum CM response to a pure-tone stimulus is expected to occur at a specific location (Bekesy 1960; Greenwood 1961; Li et al. 2021). In contrast, for CI recipients with diseased cochleae, the spatial patterns of CM amplitude display significant variability, as current studies have demonstrated (Bester et al. 2017; Harris et al. 2017; Giardina et al. 2019).

The prevalent method for ECochG analysis and interpretation involves the visual assessment by an expert (Weder et al. 2021; Bester et al. 2022). This inconsistent approach, however, hinders reproducibility and comparability between analyses across different research centers Schuerch et al. (2023a) . In addition, intracochlear measurement locations are often reported using the electrode number without accounting for the considerable variation in cochlear size and shape among individuals or variation in insertion depth. This leads to significant discrepancies in data interpretation (Schuerch et al. 2023b). Therefore, a more systematic and standardized approach is needed to improve the interpretation of ECochG measurements.

To overcome these limitations, our approach encompasses: (i) the adoption of an objective methodology that integrates model-based algorithms for the quantitative characterization of ECochG signals, as delineated in Andonie et al. (2023), and (ii) the utilization of computed tomography (CT) scans for accurately determining the exact locations of measurement electrodes, as outlined in Schraivogel et al. (2023a).

[1]Hearing Research Laboratory, ARTORG Center for Biomedical Engineering Research, Bern University Hospital, University of Bern, Bern, Switzerland; [2]Department of Otorhinolaryngology, Head & Neck Surgery, Inselspital, Bern University Hospital, University of Bern, Bern, Switzerland; and [3]Department of Otorhinolaryngology, Klinikum rechts der Isar, Technical University of Munich, Munich, Germany.

<zdoi; 10.1097/AUD.0000000000001546>

TABLE 1. Demographics of the 31 subjects examined

ID	Sex	Side	Course*	Age† (yrs)	CDL‡ (mm)	AID§ (°)	PTA¶ (dBHL)
S-01	M	R	S, T	43	36.8	358	82
S-02	F	R	S	69	35.5	328	88
S-03	F	R	P, EH	42	30.9	457	88
S-04	M	L	P, EH	57	32	437	68
S-05	M	R	P	76	35.2	393	70
S-06	F	L	P	62	31	385	105
S-06	F	R	P	62	32	385	98
S-07	F	R	S	40	34.7	394	78
S-08	M	R	P	78	32.9	456	62
S-09	M	R	S, T	28	37.4	447	108
S-10	F	R	P	48	30.6	458	105
S-11	F	R	P, EH	62	33.1	428	73
S-12	F	L	P	59	33.9	323	70
S-13	M	R	S	56	32.2	393	85
S-14	F	L	P, OS	72	32.3	434	85
S-15	M	L	S	68	35	416	73
S-16	F	R	P	79	30.1	481	102
S-17	F	R	P	87	32.1	352	100
S-18	F	L	P, OS	82	31.4	457	68
S-19	M	L	P, EH	62	34.7	398	75
S-20	F	R	S	60	31.8	422	82
S-21	M	R	P	29	35	369	65
S-22	F	R	S	65	35.5	384	48
S-23	M	R	P	85	34	302	75
S-24	M	L	P, EH	62	36.8	386	73
S-25	M	L	P	71	32.1	404	78
S-26	M	R	P	74	31.8	283	84
S-27	M	R	P	57	31.7	425	68
S-28	M	L	P, OS	80	31.2	498	58
S-29	F	R	S	38	31.1	454	85
S-30	F	L	P	54	32.1	393	94
Mean				62	33.1	403	80

*Etyology where known.
†Age at surgery.
‡Cochlear duct length.
§Angular insertion depth of the most apical electrode in degrees.
¶Pure-tone average (preoperative).
AID, angular insertion depth; CDL, cochlear duct length, EH, endolymphatic hydrops; OS, otosklerosis; P, progressive sensory-neural hearing loss; PTA, pure-tone average; S, sudden sensory-neural hearing loss; T, trauma.

We hypothesize that CM amplitudes and their spatial patterns are indicative of residual inner ear function in CI patients. By correlating these quantitative ECochG measures with exact electrode positions, we aim to deepen the understanding of ECochG amplitude patterns. This advancement is expected to facilitate a more accurate assessment of cochlear health in CI recipients.

MATERIALS AND METHODS

Patient Cohort

This prospective cohort study was conducted in accordance with the Declaration of Helsinki and has been approved by the local institutional review board. Written informed consent was obtained from all individuals before publication of any data included in this article.

We included 31 cases (ears) from 30 patients receiving a CI622 cochlear implant (Cochlear Ltd., Sydney, Australia) in our analysis. The demography of the study population is summarized in Table 1.

Residual Hearing

In an acoustic chamber, we recorded unaided air conduction pure-tone audiograms at 0.25, 0.5, 0.75, and 1 kHz using a clinical audiometer (Equinox, Interacoustics A/S, Assens, Denmark) connected to insert earphones the day before surgery. We calculated the low-frequency pure-tone average at 0.25, 0.5, and 1 kHz.

CT and Electrode Locations

We used pre- and postoperative CT scans to determine intracochlear electrode positions. For each cochlea, a reference coordinate system was computed based on manual landmark selection followed by a robust modiolar axis detection using the preoperative scans (Verbist et al. 2010; Wimmer et al. 2019). Manually selected cochlear base length A and base width B were used to estimate the cochlear duct length

$$\mathrm{CDL} = 1.71 \cdot \left(1.18 \cdot A\mathrm{oc} + 2.69 \cdot B\mathrm{oc} - \sqrt{0.72 \cdot A\mathrm{oc} \cdot B\mathrm{oc}}\right) + 0.18\ \mathrm{mm}$$

with $A\mathrm{oc} = A - 1$ mm and $B\mathrm{oc} = B - 1$ mm (Alexiades et al. 2015; Schurzig et al. 2018; Rathgeb et al. 2019; Alshalan et al. 2022; Schraivogel et al. 2023b). To ensure reproducibility, Cartesian electrode locations were visually identified in the postoperative scans that were co-registered with the preoperative scans (Schraivogel et al. 2023a). Using the reference coordinate system, the angular insertion depth and the linear insertion depth were computed for all electrodes. Based on the linear insertion depth x, we then calculated the expected tonotopic frequency

$$F_{\mathrm{T}}(x) = 165.4\ \mathrm{Hz} \cdot \left(10^{\frac{2.1 \cdot (\mathrm{CDL} - x)}{\mathrm{CDL}}} - 0.88\right)$$

for each individual electrode to assign the measured ECochG responses to their expected functional location (Greenwood 1990).

Intraoperative ECochG

For acoustic stimulation, the acoustic component of a Nucleus 6 hybrid sound processor (Cochlear Ltd.) was interfaced using a 25-cm-long sterile plastic sound delivery tube (ER3-21; Etymotic Research Inc., Elk Grove Village, IL, USA). This tube was connected to a sterile foam eartip (ER3-14A; Etymotic Research Inc.), which was positioned in the patient's outer ear canal before the surgical incision. Both the foam eartips and sound tubes were sterilized using hydrogen peroxide vapor low-temperature plasma (STERRAD 100NX, Advanced Sterilization Products [ASP], Irvine, CA, USA). After complete electrode insertion, ECochG responses were recorded using the 11 evenly numbered intracochlear electrodes of the CI. We applied 11 ms long pure-tone stimuli at 0.25, 0.5, 0.75, and 1 kHz with intensities 112, 108, 114, and 115 dBHL, respectively. Each epoch was obtained by averaging 30 measurements. The sampling rate was 20.5 kHz with a recording window of 16 ms. All measurements were performed using the Cochlear Research Platform 2.0 software (Cochlear Ltd.).

We used autonomous linear state-space models to estimate CM amplitude and response confidence from the difference signal between condensation and rarefaction phase. In this context, the CM response confidence is expressed by the logarithmic cost ratio (LCR), which compares a response model with a noise model. We excluded patients from the study if they

lacked any measurable CM response, as determined by an LCR of less than 0.35. At $\mathrm{LCR} = -1/2 \cdot \log(1/2) \approx 0.35$, observing a CM response is twice as likely as observing pure random noise (Andonie et al. 2023).

We determined the CM peak amplitudes within a measurement, which we refer to as the "CM maximum response" (CM-MR). To qualify as a CM-MR, the respective amplitude had to exceed the median of all electrodes by 30%, as suggested by Bester et al. (2017). Measurements with no peak, and therefore no CM-MR, were deemed "flat" and were excluded from further analysis.

CM amplitudes are reported in

$$\mathrm{dB}\mu\mathrm{V} = 20 \cdot \log_{10}(\text{CM amplitude voltage}/1\mu\mathrm{V}).$$

For all CM-MR, we calculated the

$$\text{octave distance} = \log_2(F_\mathrm{T}/F_\mathrm{ref})$$

between the estimated F_T at the CM-MR location and the reference frequency F_ref. Because the electrode arrays do not cover the full tonotopic frequency range examined, we assigned F_ref, the acoustic stimulation frequency F_stim, bounded by the individual tonotopic frequency range covered by the electrode array. Positive octave values denote a basal tonotopic shift of the CM-MR, negative values an apical tonotopic shift.

Statistical Analysis

We used a linear regression model to assess the relationship between CM-MR amplitudes and tonotopic shift with preoperative hearing thresholds. Correlation was assessed using Pearson's correlation coefficient r, which we reported together with its 95% confidence interval in square brackets. Statistical significance was determined by the p value of the model slope ($p < 0.05$). All statistical analyses were performed using the *Python* programming language version 3.10.12 using the *statsmodels* module version 0.14.0 (Seabold & Perktold 2010).

RESULTS

Preoperative Residual Hearing

Population results of the audiometric tests are shown in Figure 1. The median pure-tone average of the study population was 78.3 decibel hearing level (dBHL). Individual PTAs are listed in Table 1.

CT and Electrode Locations

The resolution of the CT scans varied between 0.12 and 0.37 mm with a slice thickness ranging from 0.20 to 1.50 mm. The measured CDL ranged from 30.0 to 37.4 mm with a mean of 33.1 mm. Insertion angles of the most apical electrodes were recorded in a range from 283° to 498° with a mean of 403°, as summarized in Table 1.

The linear insertion depths of the most apical electrodes ranged from 18.5 to 24.6 mm with a mean of 21.7 mm. In our cohort, the estimated tonotopic 0.25 kHz region was not reached by the most apical CI electrodes, which on average laid 5.2 mm more basally. Similarly, the 0.5 kHz region was reached only in 4 of 31 cases, with a mean distance of 1.9 mm. The.75 and 1 kHz regions, on the other hand, were surpassed in 18 and 28 cases with mean distances of −0.2 and −2.2 mm, respectively.

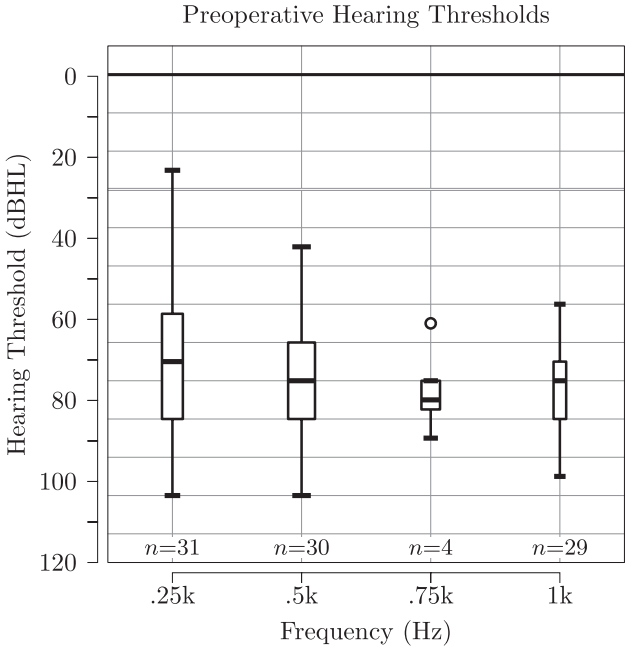

Fig. 1. Preoperative hearing thresholds of the study population. Shown are box-and-whisker diagrams in the low-frequency domain from 0.25 to 1 kHz. Median values are represented by thick lines within the boxes. The box boundaries mark the IQR while the whiskers extend to the outermost data points within the range of 1.5 × IQR. An outlier at 0.75 kHz is marked by a circle. IQR indicates interquartile range.

Intraoperative ECochG

Based on the LCR criterion, we detected ECochG responses in 31 of 36 cases, which are summarized in Table 1. A representative ECochG response is illustrated in Figure 2.

For all stimulation frequencies, CM-MR amplitudes ranged from 1.479 to 4.495 dBμV around a mean of 1.832 dBμV and a SD of 1.468 dBμV. The amplitudes were similar for all measurement frequencies, with means of 1.876, 1.696, 1.881, and 1.914 dBμV for 0.25, 0.5, 0.75, and 1 kHz, respectively. Amplitudes of the CM-MR were found to be higher in patients with better preoperative hearing. This relationship was confirmed by the linear regression analysis using 80 CM responses where valid audiometric thresholds were available, indicating a significant negative correlation between CM-MR amplitude and preoperative hearing thresholds (−7.0 dBHL per dBμV, $p < 0.001$, $r = -0.62$ $[-0.74, -0.45]$), as shown in the left panel of Figure 5.

The angular insertion depths of the CM-MR electrodes showed high variance across the study population, particularly at lower stimulation frequencies. CM-MR for lower stimulation frequencies tended to be measured more apically compared with those for higher frequencies. This trend was reflected in the mean values for each stimulation frequency, which lay in the region between 180° and 270°, as shown in Figure 3. However, applying a one-way analysis of variance, there was no statistically significant difference across the frequency groups ($p = 0.065$).

Overall frequencies, the mean tonotopic shift of the CM-MR was 1.6 octaves with a SD of 1.2 octaves. The maximum shift observed was 4.1 octaves. The mean tonotopic shifts for each frequency were also similar, namely 1.4, 1.6, 1.8, and 1.7 octaves for 0.25, 0.5, 0.75, and 1 kHz, respectively. The tonotopic shifts

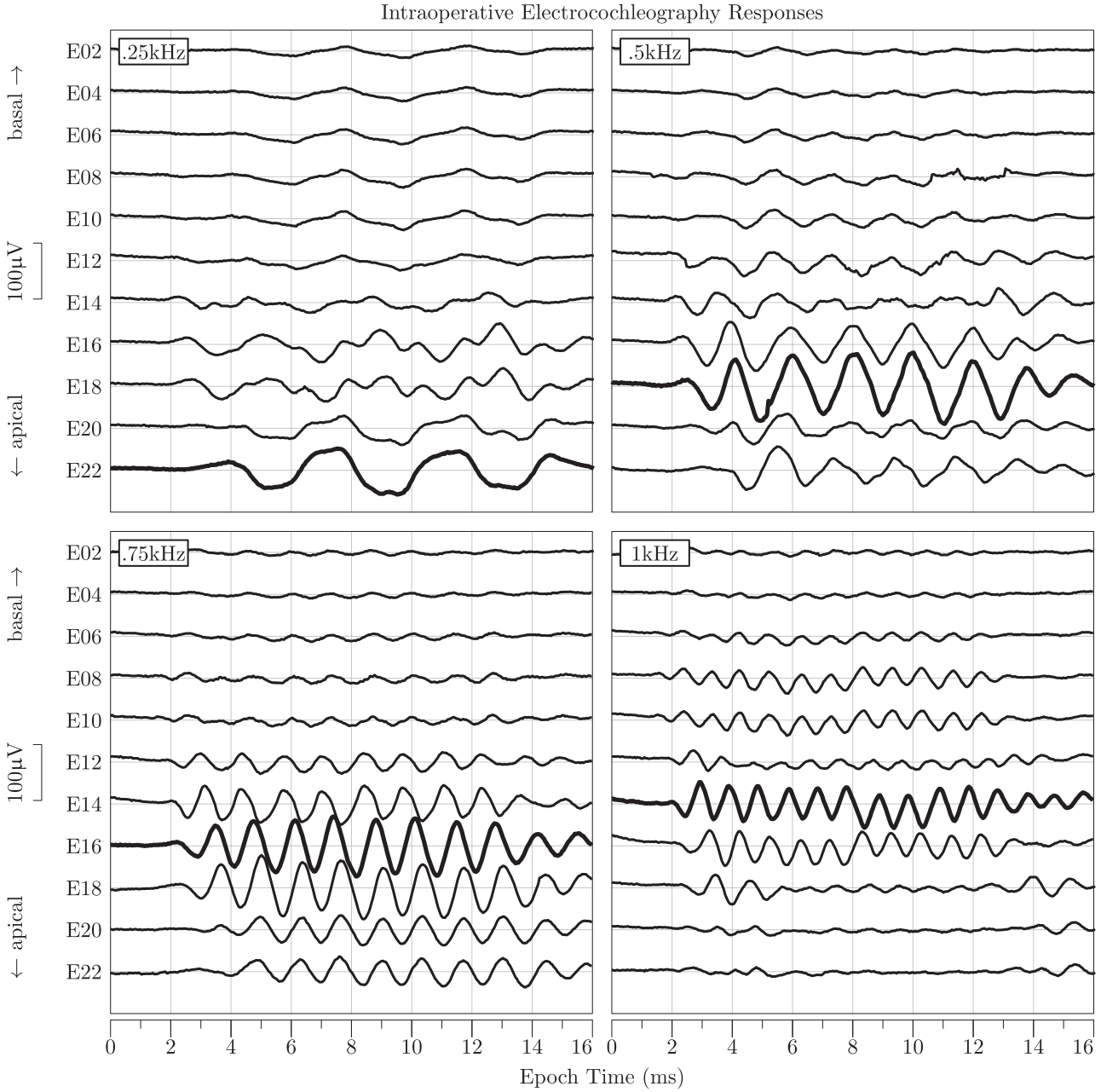

Fig. 2. Intraoperative ECochG recorded through the CI for a single patient (S-11). Shown are the raw differential signals between condensation and rarefaction phase, emphasizing the CM potential. Each panel corresponds to a specific stimulation frequency, namely 0.25, 0.5, 0.75, and 1 kHz. For each frequency, epochs are shown for every evenly numbered intracochlear E of the CI. Epochs demonstrating the CM maximum responses for each frequency are highlighted with thick lines. CI indicates cochlear implant; CM, cochlear microphonic; E, electrode; ECochG, electrocochleography.

for all cases are illustrated in Figure 4. In all but two instances (S-16 and S-28 at 0.75 kHz), the tonotopic shifts were predominantly basally directed. We found that smaller tonotopic shifts of the CM-MR were associated with better preoperative hearing thresholds. The regression analysis indicated a significant positive correlation in this context (6.2 dBHL per octave, $p < 0.001$, $r = 0.46$ [0.27, 0.62]), as shown in the right panel of Figure 5.

DISCUSSION

In our study, we used model-based algorithms to objectively assess CM responses with precise measurement locations derived from CT imaging. This methodology enabled us to establish the correlation between CM-MR amplitudes and preoperative hearing thresholds. In addition, our results indicate a connection between poor residual cochlear function and diminished CM-MR tonotopy. These insights emphasize the importance of ECochG as a biomarker for monitoring cochlear health, both during and after CI surgery.

Objective ECochG Analysis

From our perspective, the objectification of ECochG signal analysis is crucial, as it overcomes the limitations caused by

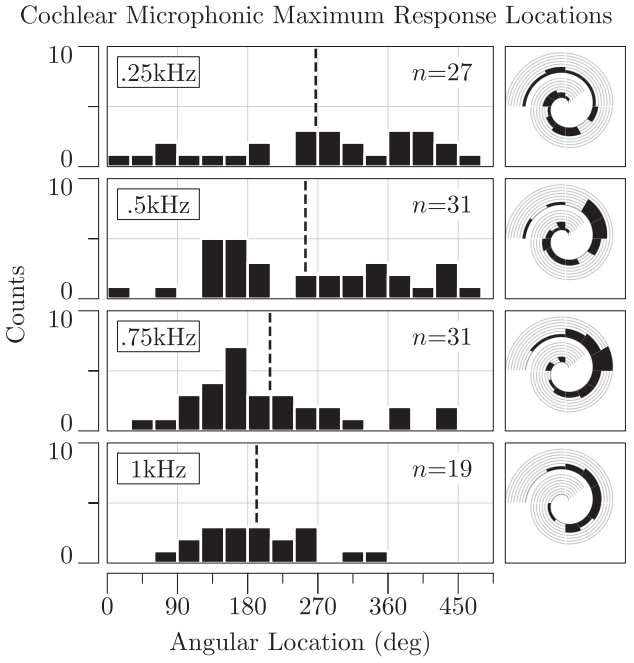

Fig. 3. Histograms showing the angular locations of the CM-MR within the cochlea. Bin width is 30°. In each row, the distribution of CM-MR for one of the stimulation frequencies, that is, 0.25, 0.5, 0.75, and 1 kHz are separately shown. In the four left panels, the angular locations are plotted on the abscissa, mean values are indicated by vertical dashed lines. In the right panels, the same histograms are plotted along a spiral resembling the cochlea. CM-MR indicates cochlear microphonic maximum responses.

visual interpretation through experts. To address this issue, we applied a previously described, objective analysis method based on Autonomous Linear State-Space Models (Andonie et al. 2023). Beyond providing an objective evaluation of ECochG signals, this methodology also offers the advantage of transparently defining inclusion criteria for patient selection. In our study, we used a predefined cut off (LCR of 0.35 or greater) to determine which patients are integrated into the final cohort analysis. This approach effectively avoids selection bias in the data analysis.

CT and Electrode Positions

Many ECochG studies only report electrode numbers instead of the actual electrode positions. This approach neglects the considerable variance in CDL and insertion depth of the electrode array, both significantly affecting the intracochlear measurement location of the ECochG. Our CT data revealed a substantial variation in CDL, with differences of up to 7.3 mm between individuals. Therefore, the incorporation of individual CDL and electrode positions is critical for the interpretation of the ECochG data. We used the continuous Greenwood's function to calculate the tonotopic shift using linear insertion depths and CDLs. Greenwood's function is a place-frequency map for the organ of Corti, which comprises the outer hair cells, the main generators of the CM potentials examined in this study (Dallos & Cheatham 1976; Greenwood 1990; Schuerch et al. 2022b). However, this is a mere approximation, and other maps like Stakhovskaya's map for the spiral ganglion are also commonly used in CI research (Stakhovskaya et al. 2007). Consequently, the use of estimated characteristic frequency locations limits the accuracy of our tonotopic shift calculations.

Residual Hearing and CM

Our analysis showed a notable correlation between intraoperative CM-MR amplitude and preoperative audiograms, aligning with findings from other researchers (Koka et al. 2017; Bester et al. 2023; Walia et al. 2023). This correlation is important as it reflects the residual inner ear function, validating CM as a biomarker for cochlear health.

Furthermore, we found an association between residual hearing and the tonotopic location of the CM-MR electrode. Moving beyond the traditional approach of categorizing CM amplitude patterns into apical peak, mid-peak, and flat patterns, our methodology enables continuous analysis across all individuals. This comprehensive approach provides a holistic view of the study population and enhances the understanding of varying ECochG responses. We observed that individuals with CM-MR locations closer to the expected tonotopic location (i.e., with a smaller tonotopic shift), tended to exhibit better residual hearing. This indicates that in cochleae with better preoperative function, a more clearly defined tonotopic organization is maintained. Conversely, in cases with poor residual hearing, this tonotopic organization appears to be compromised, likely due to inactive or absent outer hair cells. This distinction underscores the importance of tonotopic organization in understanding cochlear health and the impact of residual hearing on the interpretation of ECochG signals.

In cases where a tonotopic shift was detected, it was predominantly directed in the basal direction, irrespective of the stimulation frequency. This observation aligns with the findings reported in existing literature (Bester et al. 2023; Schuerch et al. 2023b). This has important consequences for the interpretation of ECochG data. It is assumed that the CM amplitudes for low-frequent stimuli gradually increase from base to apex and only decrease if the electrode surpasses the tonotopic region dedicated to the stimulation frequency (Honrubia & Ward 1968). In our cohort, the electrode array reached the.5 kHz tonotopic region only in 4 of 31 cases while never reaching the 0.25 kHz region. However, CM-MR angular locations showed considerable variability in our data and we would have expected the CM-MR to be recorded at the most apical electrode more consistently. Nonetheless, we observed low-frequent stimuli to yield more apically located CM-MR than stimuli of higher frequencies, even though this effect was not significant.

Similarly, in the context of continuous ECochG measurement during the electrode insertion (i.e., real-time ECochG), one would anticipate an increase in amplitude from the beginning to the end of the electrode insertion process (Calloway et al. 2014; Giardina et al. 2019; Walia et al. 2022). Current literature suggests, that a decrease in amplitude during the insertion process is primarily attributed to traumatic factors (Campbell et al. 2016; Harris et al. 2017; Dalbert et al. 2018; Giardina et al. 2018). Considering our postinsertion data, it is evident that this interpretation requires reassessment. Apart from traumatic etiology, amplitude decreases could also result from other factors influencing ECochG tonotopy, such as the fixation of the basilar membrane by the inserted electrode, high stimulation intensities, or localized dysfunction of outer hair cells within the cochlea (Ruggero 1992; Bester et al. 2020, 2023).

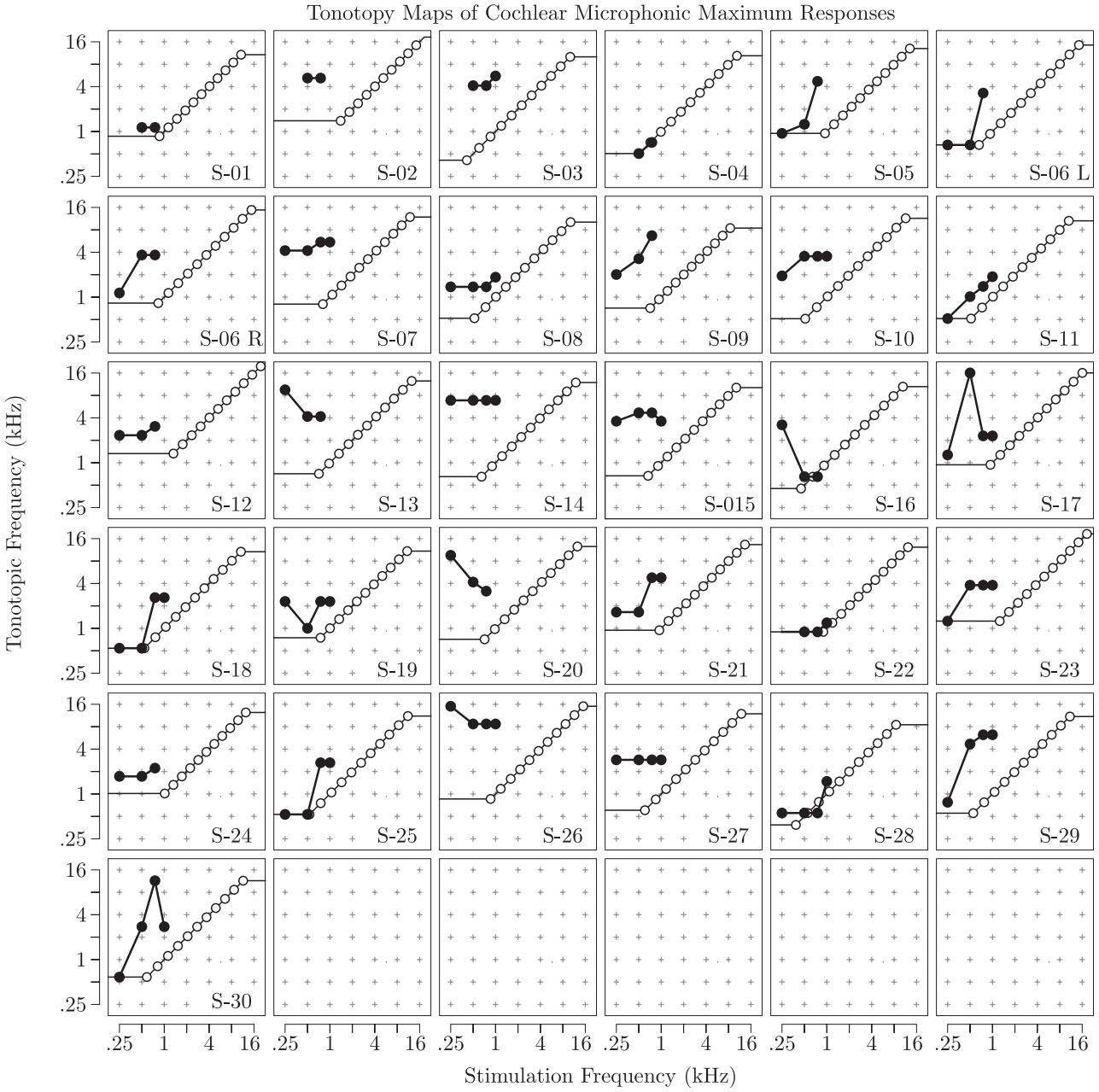

Fig. 4. Tonotopy maps from intraoperative electrocochleography. This figure illustrates the tonotopic shifts of the CM-MR for all cases, measured at four different acoustic stimulation frequencies (0.25, 0.5, 0.75, and 1 kHz). Stimulation frequencies are plotted along the abscissa, while the radiologically estimated tonotopic frequencies for each case are mapped to the ordinate. The white dots correspond to the electrode locations and mark the expected CM-MR. The connected black dots display the actual measurements. The vertical distance between the measured points and the solid reference line running through the expected points represents the tonotopic shift for the respective stimulation frequency. Tonotopic shifts are predominantly in the basal direction, as the measurements lay above the reference line. CM-MR indicates cochlear microphonic maximum responses.

Limitations

In our study, ECochG was recorded after complete electrode insertion. Real-time measurements during electrode insertion were not included in the analysis, as the movement of the electrode prevents accurate determination of the measurement location. Furthermore, the spatial resolution of the ECochG measurements was restricted by the spacing of the CI electrode array. While the analysis of discrete CM-MR locations is straightforward, a more holistic description of the CM amplitude patterns could further deepen our understanding of ECochG. In addition, the ECochG patterns need to be correlated with more variables (i.e., speech understanding scores) to understand these relationships in a broader context.

CONCLUSIONS

The combination of objective signal analysis and the consideration of intracochlear measurement locations enhances the understanding of cochlear health and overcomes the obstacles of

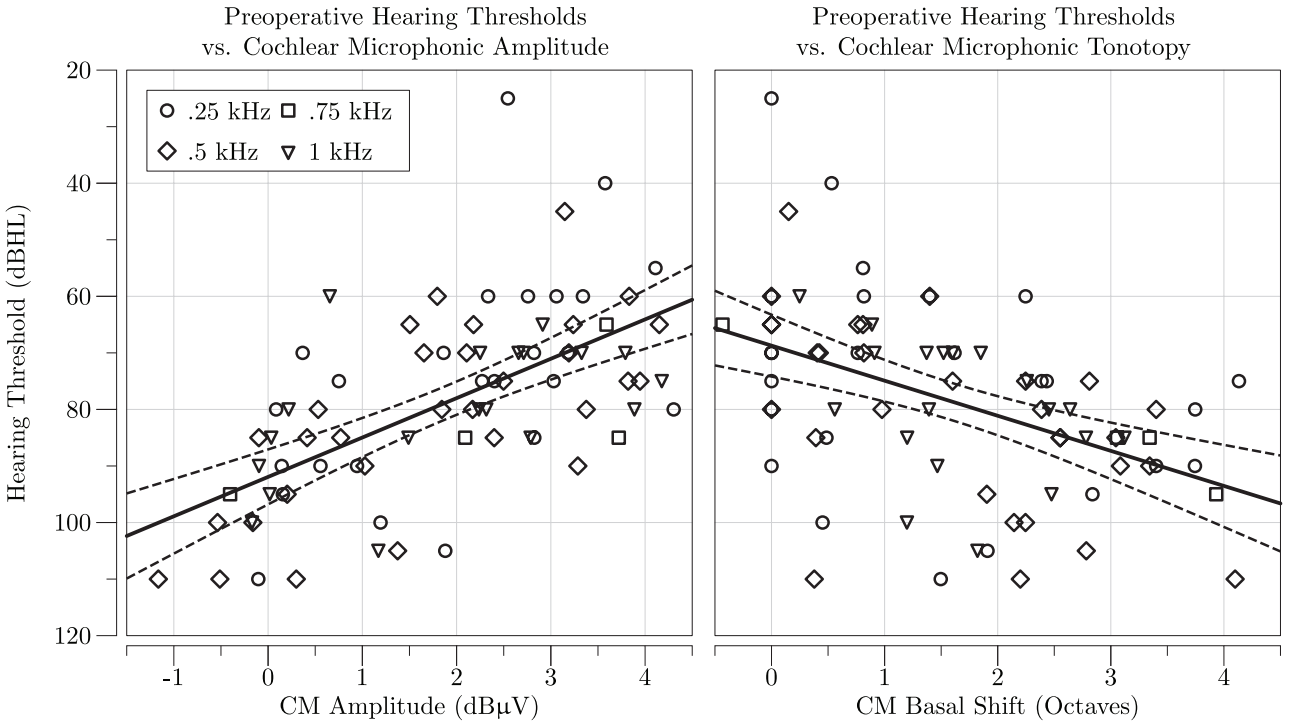

Fig. 5. Preoperative hearing thresholds vs. cochlear microphonic maximum response amplitude (left) and tonotopic shift (right). The different marker shapes correspond to the stimulation frequencies (i.e., 0.25, 0.5, 0.75, and 1 kHz). The outputs of linear regression models and their 95% confidence intervals are represented by solid and dashed lines, respectively. CM indicates cochlear microphonic.

current ECochG analysis. We discovered a link between intraoperative CM amplitudes, their spatial distributions, and preoperative hearing thresholds. Consequently, integrating these aspects has the potential to enhance the specificity of ECochG analysis, thereby reinforcing its role as an objective biomarker for cochlear health.

ACKNOWLEDGMENTS

This work was supported in part by Cochlear Ltd., Sydney, Australia, and the Department of Otorhinolaryngology of the Bern University Hospital, Inselspital. The authors declare that they have no competing financial interests or personal relationships that could have influenced the work reported in this paper.

R. R. A.: Conceptualization, methodology, formal analysis, measurements and data curation, writing-original draft; W. W.: Conceptualization, methodology, measurements and data curation, formal analysis, writing-review & editing; S. S.: Methodology, writing-review and editing; G. M.: Measurements, writing-review and editing; M .C.: Resources, Writing-review & editing; S. W.: Conceptualization, supervision and project administration, measurements, writing-original draft; all authors contributed to the article and approved the submitted version.

The measurement data would be made available upon request to the authors after a formal data-sharing agreement has been reached.

This study was conducted in accordance with the Declaration of Helsinki and has been approved by the local institutional review board (KEK-Bern, Switzerland. BASEC number 2019-01578).

The authors have no conflicts of interest to disclose.

Address for correspondence: Stefan Weder, Department of Otorhinolaryngology, Head & Neck Surgery, Inselspital, Bern University Hospital, University of Bern, Bern 3008, Switzerland. E-mail: stefan.weder@insel.ch

Received January 15, 2024; accepted June 02, 2024

REFERENCES

Alexiades, G., Dhanasingh, A., Jolly, C. (2015). Method to estimate the complete and two-turn cochlear duct length. *Otol Neurotol*, *36*, 904–907.

Alshalan, A., Abdelsamad, Y., Assiri, M., Alsanosi, A. (2022). Cochlear implantation: The variation in cochlear height. *Ear Nose Throat J*, *0*, 1455613221134860.

Andonie, R. R., Wimmer, W., Wildhaber, R. A., Caversaccio, M., Weder, S. (2023). Real-time feature extraction from electrocochleography with impedance measurements during cochlear implantation using linear state-space models. *IEEE Trans Biomed Eng*, *70*, 3137–3146.

Bester, C. W., Campbell, L., Dragovic, A., Collins, A., O'Leary, S. J. (2017). Characterizing electrocochleography in cochlear implant recipients with residual low-frequency hearing. *Front Neurosci*, *11*, 141.

Bester, C., Collins, A., Razmovski, T., Weder, S., Briggs, R. J., Wei, B., Zakaria, A. F., Gerard, J. -M., Mitchell-Innes, A., Tykocinski, M., Kennedy, R., Iseli, C., Dahm, M., Ellul, S., O'Leary, S. (2022). Electrocochleography triggered intervention successfully preserves residual hearing during cochlear implantation: Results of a randomised clinical trial. *Hear Res*, *426*, 108353.

Bester, C., Dalbert, A., Collins, A., Razmovski, T., Gerard, J. M., O'Leary, S. (2023). electrocochleographic patterns predicting increased impedances and hearing loss after cochlear implantation. *Ear Hear*, *44*, 710–720.

Bester, C., Weder, S., Collins, A., Dragovic, A., Brody, K., Hampson, A., O'Leary, S. (2020). Cochlear microphonic latency predicts outer hair cell function in animal models and clinical populations. *Hear Res*, *398*, 108094.

Calloway, N. H., Fitzpatrick, D. C., Campbell, A. P., Iseli, C., Pulver, S., Buchman, C. A., Adunka, O. F. (2014). Intracochlear electrocochleography during cochlear implantation. *Otol Neurotol*, *35*, 1451–1457.

Campbell, L., Kaicer, A., Sly, D., Iseli, C., Wei, B., Briggs, R., O'Leary, S. (2016). Intraoperative real-time cochlear response telemetry predicts hearing preservation in cochlear implantation. *Otol Neurotol*, *37*, 332–338.

Dalbert, A., Pfiffner, F., Hoesli, M., Koka, K., Veraguth, D., Roosli, C., Huber, A. (2018). Assessment of cochlear function during cochlear implantation by extra- and intracochlear electrocochleography. *Front Neurosci*, *12*, 18.

Dallos, P., Billone, M. C., Durrant, J. D., Wang, C., Raynor, S. (1972). Cochlear inner and outer hair cells: Functional differences. *Science*, *177*, 356–358.

Dallos, P., & Cheatham, M. A. (1976). Production of cochlear potentials by inner and outer hair cells. *J Acoust Soc Am*, *60*, 510–512.

Gantz, B. J., Hansen, M., Dunn, C. C. (2022). Review: Clinical perspective on hearing preservation in cochlear implantation, the University of Iowa experience. *Hear Res*, *426*, 108487.

Giardina, C. K., Brown, K. D., Adunka, O. F., Buchman, C. A., Hutson, K. A., Pillsbury, H. C., Fitzpatrick, D. C. (2019). Intracochlear electrocochleography: Response patterns during cochlear implantation and hearing preservation. *Ear Hear*, *40*, 833–848.

Giardina, C. K., Khan, T. E., Pulver, S. H., Adunka, O. F., Buchman, C. A., Brown, K. D., Pillsbury, H. C., Fitzpatrick, D. C. (2018). Response changes during insertion of a cochlear implant using extracochlear electrocochleography. *Ear Hear*, *39*, 1146–1156.

Gifford, R. H., Dorman, M. F., Skarzynski, H., Lorens, A., Polak, M., Driscoll, C. L., Roland, P., Buchman, C. A. (2013). Cochlear implantation with hearing preservation yields significant benefit for speech recognition in complex listening environments. *Ear Hear*, *34*, 413–425.

Greenwood, D. D. (1961). Critical bandwidth and the frequency coordinates of the basilar membrane. *J Acoust Soc Am*, *33*, 1344–1356.

Greenwood, D. D. (1990). A cochlear frequency-position function for several species–29 years later. *J Acoust Soc Am*, *87*, 2592–2605.

Harris, M. S., Riggs, W. J., Giardina, C. K., O'Connell, B. P., Holder, J. T., Dwyer, R. T., Koka, K., Labadie, R. F., Fitzpatrick, D. C., Adunka, O. F. (2017). Patterns seen during electrode insertion using intracochlear electrocochleography obtained directly through a cochlear implant. *Otol Neurotol*, *38*, 1415–1420.

Hempel, J. M., Simon, F., ller, J. M. (2018). Extended applications for cochlear implantation. *Adv Otorhinolaryngol*, *81*, 74–80.

Honrubia, V., & Ward, P. H. (1968). Longitudinal distribution of the cochlear microphonics inside the cochlear duct (guinea pig). *J Acoust Soc Am*, *44*, 951–958.

Koka, K., Saoji, A. A., Litvak, L. M. (2017). Electrocochleography in cochlear implant recipients with residual hearing: Comparison with audiometric thresholds. *Ear Hear*, *38*, e161–e167.

Lenarz, T., Buechner, A., Gantz, B., Hansen, M., Tejani, V. D., Labadie, R., O'Connell, B., Buchman, C. A., Valenzuela, C. V., Adunka, O. F., Harris, M. S., Riggs, W. J., Fitzpatrick, D., Koka, K. (2022). Relationship between intraoperative electrocochleography and hearing preservation. *Otol Neurotol*, *43*, e72–e78.

Li, H., Helpard, L., Ekeroot, J., Rohani, S. A., Zhu, N., Rask-Andersen, H., Ladak, H. M., Agrawal, S. (2021). Three-dimensional tonotopic mapping of the human cochlea based on synchrotron radiation phase-contrast imaging. *Sci Rep*, *11*, 4437.

Rathgeb, C., Demattè, M., Yacoub, A., Anschuetz, L., Wagner, F., Mantokoudis, G., Caversaccio, M., Wimmer, W. (2019). Clinical applicability of a preoperative angular insertion depth prediction method for cochlear implantation. *Otol Neurotol*, *40*, 1011–1017.

Ruggero, M. A. (1992). Responses to sound of the basilar membrane of the mammalian cochlea. *Curr Opin Neurobiol*, *2*, 449–456.

Schraivogel, S., Aebischer, P., Wagner, F., Weder, S., Mantokoudis, G., Caversaccio, M., Wimmer, W. (2023a). Postoperative impedance-based estimation of cochlear implant electrode insertion depth. *Ear Hear*, *44*, 1379–1388.

Schraivogel, S., Aebischer, P., Weder, S., Caversaccio, M., Wimmer, W. (2023b). Cochlear implant electrode impedance subcomponents as biomarker for residual hearing. *Front Neurol*, *14*, 1183116.

Schuerch, K., Waser, M., Mantokoudis, G., Anschuetz, L., Wimmer, W., Caversaccio, M., Weder, S. (2022a). Performing intracochlear electrocochleography during cochlear implantation. *J Vis Exp*.

Schuerch, K., Wimmer, W., Dalbert, A., Rummel, C., Caversaccio, M., Mantokoudis, G., Gawliczek, T., Weder, S. (2023a). An intracochlear electrocochleography dataset—from raw data to objective analysis using deep learning. *Sci Data*, *10*, 157.

Schuerch, K., Wimmer, W., Dalbert, A., Rummel, C., Caversaccio, M., Mantokoudis, G., Weder, S. (2022b). Objectification of intracochlear electrocochleography using machine learning. *Front Neurol*, *13*, 943816.

Schuerch, K., Wimmer, W., Rummel, C., Caversaccio, M. D., Weder, S. (2023b). Objective evaluation of intracochlear electrocochleography: Repeatability, thresholds, and tonotopic patterns. *Front Neurol*, *14*, 1181539.

Schurzig, D., Timm, M. E., Batsoulis, C., Salcher, R., Sieber, D., Jolly, C., Lenarz, T., Zoka-Assadi, M. (2018). A novel method for clinical cochlear duct length estimation toward patient-specific cochlear implant selection. *OTO Open*, *2*, 2473974–X18800238.

Seabold, S., & Perktold J. (2010). Statsmodels: Econometric and statistical modeling with python. In 9th Python in Science Conference.

Sheffield, S. W., Jahn, K., Gifford, R. H. (2015). Preserved acoustic hearing in cochlear implantation improves speech perception. *J Am Acad Audiol*, *26*, 145–154.

Stakhovskaya, O., Sridhar, D., Bonham, B. H., Leake, P. A. (2007). Frequency map for the human cochlear spiral ganglion: Implications for cochlear implants. *J Assoc Res Otolaryngol*, *8*, 220–233.

Verbist, B. M., Skinner, M. W., Cohen, L. T., Leake, P. A., James, C., Boëx, C., Holden, T. A., Finley, C. C., Roland, P. S., Roland, J. T. Jr, Haller, M., Patrick, J. F., Jolly, C. N., Faltys, M. A., Briaire, J. J., Frijns. (2010). Consensus panel on a cochlear coordinate system applicable in histologic, physiologic, and radiologic studies of the human cochlea. *Otol Neurotol*, *31*, 722–730.

von Békésy, G. 1960. *Experiments in Hearing*. McGraw-Hill Series in Psychology. McGraw-Hill.

Walia, A., Shew, M. A., Lefler, S. M., Kallogjeri, D., Wick, C. C., Holden, T. A., Durakovic, N., Ortmann, A. J., Herzog, J. A., Buchman, C. A. (2022). Is characteristic frequency limiting real-time electrocochleography during cochlear implantation? *Front Neurosci*, *16*, 915302.

Walia, A., Shew, M. A., Varghese, J., Ioerger, P., Lefler, S. M., Ortmann, A. J., Herzog, J. A., Buchman, C. A. (2023). Improved cochlear implant performance estimation using tonotopic-based electrocochleography. *JAMA Otolaryngol Head Neck Surg*, *149*, 1120–1129.

Weder, S., Bester, C., Collins, A., Shaul, C., Briggs, R. J., O'Leary, S. (2020). Toward a better understanding of electrocochleography. *Ear Hear*, *41*, 1560–1567.

Weder, S., Bester, C., Collins, A., Shaul, C., Briggs, R. J., O'Leary, S. (2021). Real time monitoring during cochlear implantation: Increasing the accuracy of predicting residual hearing outcomes. *Otol Neurotol*, *42*, e1030–e1036.

Wimmer, W., Vandersteen C., Guevara N., Caversaccio, M., Delingette H. (2019). Robust Cochlear Modiolar Axis Detection in Ct. In International Conference on Medical Image Computing and Computer-Assisted Intervention, 3–10. Springer.